

AD-A038 938

DENVER UNIV COLO DEPT OF PHYSICS AND ASTRONOMY

F/G 4/1

ION SAMPLING THROUGH SMALL ORIFICES AS RELATED TO STRATOSPHERIC--ETC(U)

MAR 77 B V ZYL, D G MURCRAY, R C AMME

DAAG27-76-G-0122

UNCLASSIFIED

ARO-13633.1-6SX

NL

1 OF 1
AD
A038938



020-13633. 1-65X

Ion Sampling Through Small Orifices
As Related To Stratospheric Measurements

12
NW

ADA 038938

Final Report

15 December 1975 - 14 December 1976

Bert Van Zyl, David G. Murcray and Robert C. Amme

March 1977

U. S. Army Research Office

Grant No. DAAG29-76-G-0122

Department of Physics and Astronomy
University of Denver
Denver, Colorado 80208

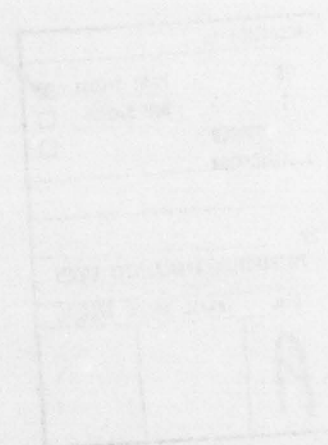
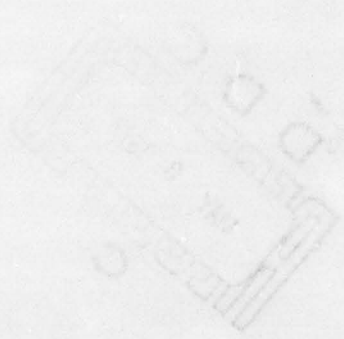
DDC
RECEIVED
MAY 3 1977
C

DDC FILE COPY

ACCESSION for	
IS	White Section <input checked="" type="checkbox"/>
;	Butt Section <input type="checkbox"/>
OUNCED	<input type="checkbox"/>
JUSTIFICATION	
BY	
DISTRIBUTION/AVAILABILITY CODES	
Dist.	AVAIL. and/or SPECIAL
A	

Approved for Public Release;
Distribution Unlimited.

THE FINDINGS IN THIS REPORT ARE NOT TO BE
CONSTRUED AS AN OFFICIAL DEPARTMENT OF
THE ARMY POSITION, UNLESS SO DESIGNATED
BY OTHER AUTHORIZED DOCUMENTS.



830880/ADH
DDC LIFE 0054

Unclassified

SECURITY CLASSIFICATION OF THIS PAGE (When Data Entered)

REPORT DOCUMENTATION PAGE		READ INSTRUCTIONS BEFORE COMPLETING FORM
1. REPORT NUMBER	2. GOVT ACCESSION NO.	3. RECIPIENT'S CATALOG NUMBER
4. TITLE (and Subtitle) Ion Sampling Through Small Orifices as Related To Stratospheric Measurements		5. TYPE OF REPORT & PERIOD COVERED Final Report 15 Dec 75 - 14 Dec 76
7. AUTHOR(s) Bert Van/Zyl, David G. Murcray, Robert C. Amme		8. CONTRACT OR GRANT NUMBER(s) DAAG27-76-G-0122
9. PERFORMING ORGANIZATION NAME AND ADDRESS Department of Physics and Astronomy University of Denver Denver, Colorado 80208		10. PROGRAM ELEMENT, PROJECT, TASK AREA & WORK UNIT NUMBERS
11. CONTROLLING OFFICE NAME AND ADDRESS U.S. Army Research Office Post Office Box 12211 Research Triangle Park, NC 27709		12. REPORT DATE March 1977
14. MONITORING AGENCY NAME & ADDRESS (if different from Controlling Office) ARO 13633.1-GSX		13. NUMBER OF PAGES 43
		15. SECURITY CLASS. (of this report) Unclassified
		15a. DECLASSIFICATION/DOWNGRADING SCHEDULE NA
16. DISTRIBUTION STATEMENT (of this Report) Approved for public release; distribution unlimited.		
17. DISTRIBUTION STATEMENT (of the abstract entered in Block 20, if different from Report) NA		
18. SUPPLEMENTARY NOTES The findings of this report are not to be construed as an official Department of the Army position, unless so designated by other authorized documents.		
19. KEY WORDS (Continue on reverse side if necessary and identify by block number) Atmospheric ions Mass Spectrometry Ion Sampling Stratosphere Ion Clusters		
20. ABSTRACT (Continue on reverse side if necessary and identify by block number) An experimental laboratory apparatus has been assembled to study the problem of sampling of low density ions from the stratosphere. The ion sampling effi- ciency was found not to depend strongly on the sampling orifice configuration or material of construction, and scaled in proportion to the orifice area. A model including the effects of ion diffusion to the sampling orifice plate is suggested to account for the low sampling efficiency observed. The apparatus was also used to develop an ion optical lens system for use in a stratospheric ion mea- surement package.		

DD FORM 1 JAN 73 1473

EDITION OF 1 NOV 68 IS OBSOLETE
S/N 0102-014-66011

Unclassified

SECURITY CLASSIFICATION OF THIS PAGE (When Data Entered)

409 002

13

TABLE OF CONTENTS

I.	Introduction	1
II.	The Laboratory Ion-Sampling Apparatus	3
III.	The Initial Measurements	8
IV.	Analysis of The Ion Sampling Rate	18
V.	The Ion Optical System and Quadrupole Mass Spectrometer	30
VI.	Summary and Discussion	33
VII.	Appendix	35
VIII.	References and Footnotes	38
IX.	Personnel	40

I. INTRODUCTION

The University of Denver, under support by the United States Army,¹ is involved in an experimental research program to observe and identify stratospheric ions with a balloon-borne mass spectrometer. This effort, initiated in December, 1972, has included the design, construction, and laboratory testing of the required flight instrument packages and, together with Army scientists, the actual flight operation of the experiments. The first instrument package constructed, which met with catastrophic destruction in September, 1975,² has been described.³ The second instrument package has only recently been completed and has made only one engineering flight to date. Some discussion of this apparatus will be presented later in this report.

The in situ observation of ions in the stratosphere is by no means a trivial task. In the first place, the expected ion density⁴ at an altitude of about 40 km is only of the order of 10^3 ions/cm³, while the corresponding neutral density is here about 10^{17} neutrals/cm³. These figures dictate the use of a highly efficient ion detection system, and one which will operate with a large neutral gas flow throughput capability. Second, ion species of the type $H^+(H_2O)_n$ (i.e., hydrated protons with "n" in the range of 2 to 6) are expected to be the major species present in the stratosphere⁴ in the altitude range of interest. Such highly clustered species are only weakly bound, and the ion sampling system must thus be operated in such a way as to minimize the destruction of these clusters during their detection. Finally, the "ion sampling orifice" must allow transmission of a large and known fraction of the ambient ion concentration. The present indications are that it is this last criterion which may be the most difficult to satisfy.

Preliminary laboratory studies made with the first flight instrument package seemed to indicate that the overall ion sampling efficiency was orders of magnitude smaller than the initial (and crudely obtained) expectation. As the difficulty did not appear to be unique to the University

of Denver experiment,⁵ it was decided to propose a laboratory study of the ion sampling process. That is, can ions be made to pass from a 2 Torr region to a high vacuum region through a small orifice under the influence of the neutral gas flow through the orifice?

This report describes the results of these studies which were undertaken with United States Army support (ARO Grant #DAAG29-76-G-0122). The proposal to ARO for these studies outlined a program of systematic investigation of the ion transmission through small apertures as functions of such parameters as orifice material, orifice diameter, orifice thickness, sampling pressure, draw-in potential, and ion concentration.

Many such studies were performed, some of which will be reviewed in Section III of this report. It was soon found, however, that the low ion sampling efficiency suspected from the preliminary studies made with the flight instrument was real, but could not be traced to any poor choices in terms of the orifice parameters listed above. That is, the behavior of the ion transmission was not critically dependent on the orifice material or configuration and behaved in about the expected way with orifice diameter.

As the prime motivation for these studies was to provide information to support the stratospheric ion density measurements, a decision was made to search for the source of the low sampling efficiency problem rather than to pursue the initial program goals in more detail. This search was begun with a moderately extensive empirical analysis of the ion sampling problem. This analysis led to a possible explanation of the ion sampling observations, at least in a qualitative way. The results of this study are summarized in Section IV of this report.

The final task undertaken as a part of these studies was an evaluation and optimization of the electrostatic ion optics required to move the ions from the ion sampling orifice to the quadrupole mass spectrometer/particle multiplier detector. A simple and yet remarkably efficient

ion-optical focusing lens system resulted from these studies and was, in fact, incorporated directly into the second flight instrument. A discussion of this system and some of its performance specifications is presented in Section V. Also included here is a typical "mass scan" obtained with the total laboratory ion sampling system.

Section VI contains a summary of the efforts of this program, indicates areas in which the laboratory evaluations have made contributions to the total flight program effort, and describes additional laboratory work which should be helpful to the overall program. Attention is now directed to a brief description of the laboratory apparatus which was assembled for these investigations.

II. THE LABORATORY ION-SAMPLING APPARATUS

The in situ sampling of ions in the stratosphere is accomplished by the flight instrument package by drawing into the instrument a small volume of the atmosphere and observing the ions present in the volume. Observation and identification of the ionic species is made with a quadrupole mass spectrometer/particle multiplier detector operating in a high-vacuum environment. The problem thus becomes one of establishing a total system efficiency, i.e., the relationship between the detector counting rate and the unperturbed ion density in the stratosphere.

In the assembly of an experimental apparatus to be used to investigate the ion sampling problem in some detail, two criteria were deemed to be of considerable importance. First, the experimental configuration used for the study should be very similar if not identical to the actual flight instrument configuration, at least in those areas pertinent to the ion sampling procedure. Second, the apparatus should be simple and easy to work with and modify, and should be one which could be put into operation as soon as possible.

This latter requirement prohibited construction of a new vacuum system facility specifically for these studies. Instead, an existing vacuum

tank, about 32 cm diameter and 22 cm deep, was used. This stainless steel chamber was fitted with a 15 cm diameter mercury diffusion pump, cold baffle, liquid nitrogen trap, and main vacuum valve, items borrowed from other experiments in the laboratory. A forepump was also made available, as was a capacitance diaphragm manometer and other pressure measurement instrumentation. Thus, with the exception of the "plumbing" and fabrication of some special vacuum flanges to fit the vacuum system ports (for the specific needs of these studies), the basic vacuum apparatus was quickly made available. Pressures of order 10^{-6} Torr were easily reached with the system in a few hours' pumping, and although the system was not of optimum configuration for this work, it did satisfy most of the basic needs of the program.

The basic components of the laboratory ion sampling system itself are shown in Fig. 1. All these components are, of course, contained in the vacuum tank described above. At the left is situated a "high pressure sampling cell" in which the pressure can be adjusted between about 1 and 100 Torr to simulate various altitudes in the atmosphere. Within this cell is an Am^{241} alpha particle emitter which is used as a source of ionization for the studies undertaken here. This source has an activity level of 700 microcuries, producing about 2.6×10^7 alpha particles/sec, with an energy of about 5.5 meV. The position and orientation of this source within the cell could be easily modified, as could the positions and orientations of various other electrodes within the cell (not shown) to accomplish a variety of measurements and tests. The potential of the source, any auxiliary electrodes, and the orifice plate itself could be controlled externally.

The pressure in the main vacuum tank was typically between four and five orders of magnitude smaller than that in the sampling cell, depending on the orifice size under investigation. As the gas flowed from the sampling cell into the main vacuum tank, it rapidly expanded into the conical shaped region beyond the orifice. Ions, swept along with this flowing gas, soon find themselves in a "long mean free path" condition, where

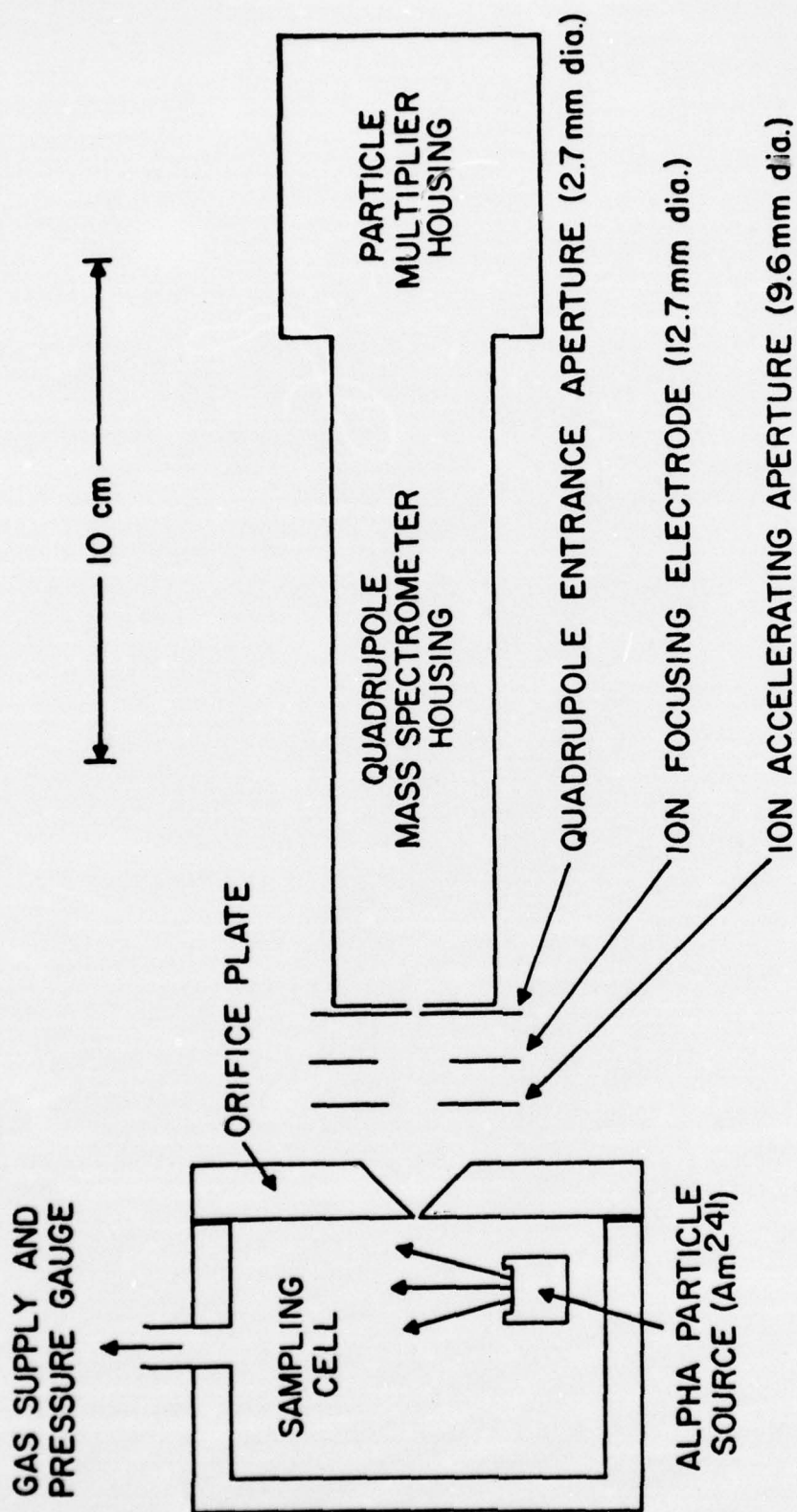


FIG. 1. The basic components of the laboratory ion sampling system

they can be electrostatically accelerated, collimated, and focused into the entrance aperture of the mass spectrometer. Provided they are of the quadrupole selected mass, the ions then traverse the spectrometer, are accelerated to several keV, and are counted by an open-faced particle multiplier.

The details of two "typical" sampling orifices are shown in Fig. 2. In 2a is found a cross section of a machined⁶ orifice and in 2b a cross section of an orifice which has been spotwelded into the orifice plate. In the latter case, the orifices were drilled or punched in thin sheet metal disks before spotwelding. After insertion, the entire orifice/orifice plate assembly was sometimes coated to insure a continuity of surface conditions in the vicinity of the hole.

The orifice plate materials used were hardened steel, stainless steel, and tungsten carbide.⁷ Separate orifices from nickel and molybdenum were tried, in most cases plated with chromium or sputtered with molybdenum after their installation. Detailed studies were not made with the laboratory ion sampling system on all these orifices, but enough data were obtained from the overall program to suggest that the choice of material or the details of the orifice shape and configuration did not have a gross effect on the sampling efficiency.

The ion optical system, composed of the electrodes between and including the orifice plate and quadrupole entrance aperture, resulted from study of several different configurations. The configuration shown in Fig. 1, which will be described in more detail in Section V, was quite efficient and simple to construct and could be operated with only a few required electrical potentials. In fact, some of the potentials used were made identical to other potentials required in the flight instrument package. The reduction in complexity and weight of the flight instrument constituted a secondary goal in terms of the development of any items for the package.

For many of the studies undertaken during this research effort, the ion optical system followed by the mass spectrometer/multiplier detector

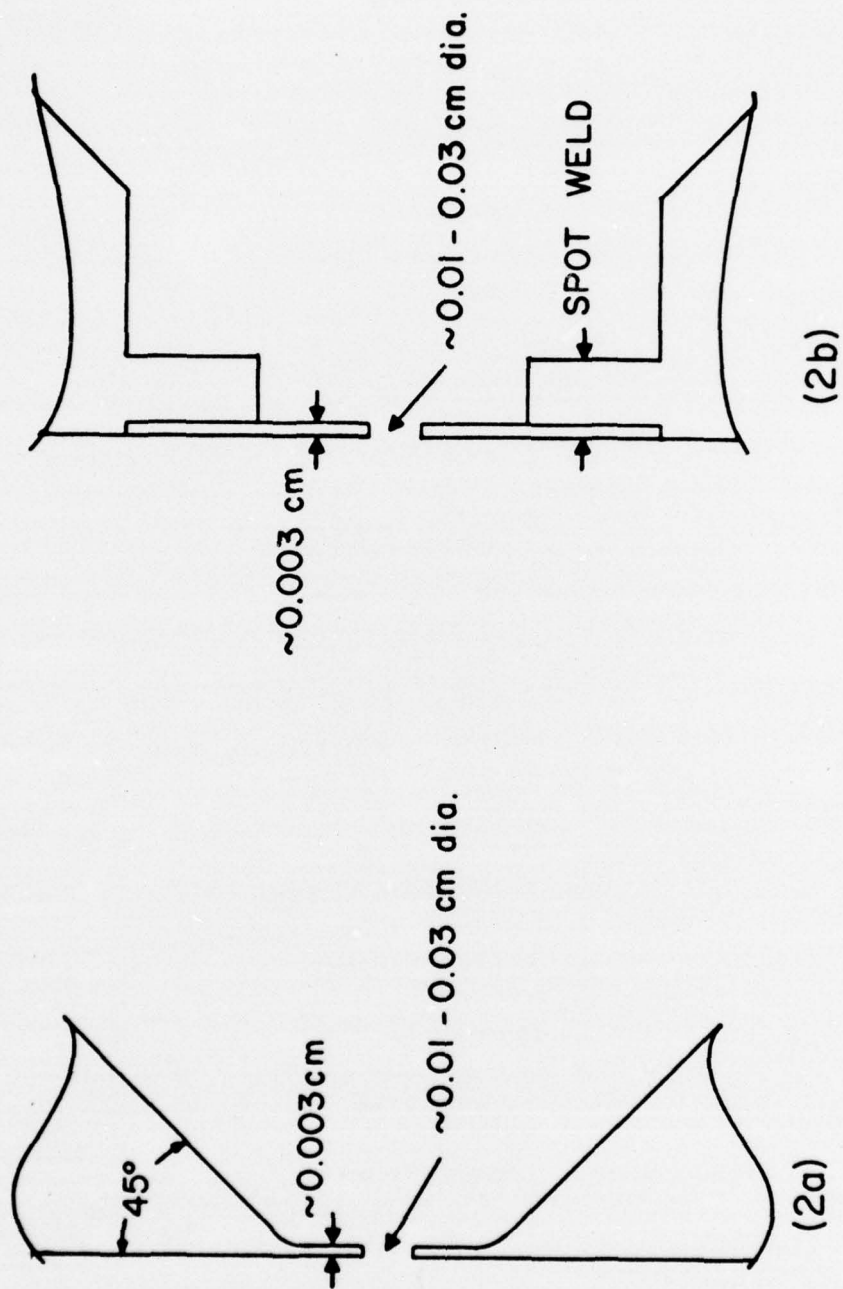


FIG. 2. Typical ion sampling orifice configurations

were not employed. Rather, it was of interest to determine the total flux of entering ions as a function of sampling cell pressure, for example, or as a function of orifice material. For such investigations, the entire electrode structure was replaced with a highly transparent grid-guarded Faraday cup ion collector just after the orifice plate. Various types of Faraday cups were also used to collect ions which had traversed one aperture or another to determine various ion collection and focus efficiencies.

All these various electrode structures were made specifically for the purpose of these studies as were the electrode supports and a new "table" to sit inside the vacuum tank. The mechanical aspects of the system allowed the components to be changed quickly and yet preserve the coaxial alignment symmetry along the axis of the sampling configuration. The various power supplies, electrometers, and quadrupole electronics for making the studies reported here were borrowed from other experiments underway in this laboratory. Thus the "apparatus and equipment" demands on the grant were not extensive and it was possible to get the investigation going at an early time. The early findings of the program are now reviewed.

III. THE INITIAL MEASUREMENTS

Most of the early measurements made as part of this research effort were directed at investigating the total number of ions traversing the orifice as a function of the sampling cell pressure. To obtain these data, a Faraday cup was used to replace the ion optics/mass spectrometer/multiplier detector combination shown in Fig. 1. Immediately in front of the Faraday cup was a highly transparent fine-screen grid. This grid was used to slightly accelerate the entering positive ions to the Faraday cup collector and to suppress any secondary electrons liberated at the collector surface. (It was also possible to use the grid to "retard" the entering ions, thereby providing a crude measure of the entering ion energy.)

The results of a typical such study are shown in Fig. 3, where the current of positive ions is plotted as a function of the sampling cell pressure. As noted, this study was made in N_2 gas with a chrome plated orifice/orifice plate surface. The orifice diameter was about 110 microns.⁸

Note that the measured ion current entering the sampling cell is not a strong function of pressure in the region above about 40 to 50 Torr. Below this pressure, however, the current begins to drop off more and more rapidly with decreasing pressure and seems to be approaching about a cubic pressure dependence below 10 Torr or so. The sensitivity limit during these early investigations was about 10^{-14} amp, the measurement data below this value being dominated by electrical noise. While the results in Fig. 3 extend up to about 100 Torr, it was, in general, not possible to go to this high a pressure unless the smaller aperture diameters were being investigated. Indeed, even for these data, the pumping system was being operated under an excessive gas load.

A very crude estimate of the number of ions per second expected to enter the high vacuum region at about 40 Torr sampling cell pressure (the procedures used in making such estimates will be reviewed in the next section), gives an entering ion current about twice as large as that actually observed at this pressure. This kind of relative agreement is clearly within the uncertainty of the crude prediction and is taken to be satisfactory. On the other hand, the rapid fall-off of the entering ion current with sampling cell pressure in the 10 Torr region was initially unexpected.

It had always been felt that the efficiency for transmission of ions through the orifice would fall off rapidly in the pressure region where the ion mean-free-path became of the same order as the orifice diameter or larger. In this low pressure region, it is difficult for an ion to negotiate the orifice without contacting the orifice plate surface during its approach to or transit through the orifice. This low pressure condition (which is basically the condition for establishing molecular flow through

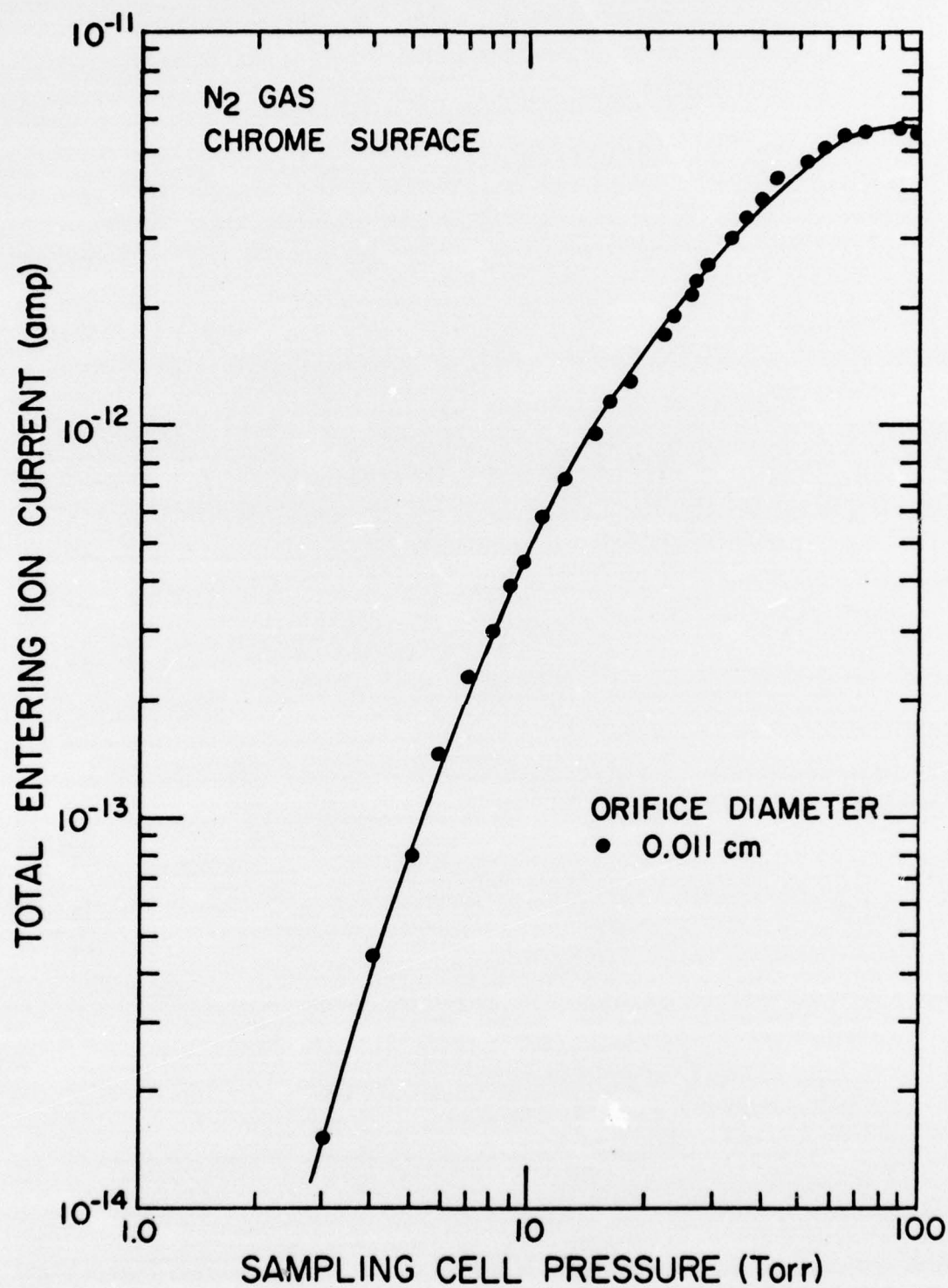


FIG. 3. Ion sampling current versus sampling cell pressure

the orifice) should apply to the region below about 1 Torr in Figure 3. Thus the rapid fall-off of the measured ion current with pressure in the 10 Torr region occurs at about an order of magnitude higher pressure than our initial (and as before, very crudely obtained) expectations.

The disturbing thing about this finding was the fact that the first flight instrument was designed to fly at about 40 km where the atmospheric pressure is of the order of 2 Torr. At this pressure, the entering ion current shown by the data of Fig. 3 fell more than 2 orders of magnitude below what had been initially expected. There was little question but that this type of behavior was also responsible for the essential lack of ions observed when this first flight instrument was tested in the laboratory.⁹

It was initially postulated that the rapid fall-off of entering ion current with pressure such as exhibited by Fig. 3 was the result of some sort of surface/electrical phenomenon. That is, it was felt that the surface in the vicinity of the orifice sat at some effective potential relative to the "at rest" potential energy of a sampling cell ion, and this potential barrier was prohibiting the ions from entering the immediate orifice region.¹⁰ Such phenomena as contact potentials, electrochemical potentials, and ion image-charge potentials were invoked to explain the results.

One "model" that received some early attention was that the effective cross sectional area of the orifice was being reduced by some electro-surface phenomenon such as mentioned above. If one accepts the fact that the surface in the orifice vicinity may be charged, a "forbidden zone" for ions near the surface can be postulated such that any ion finding itself within some critical distance from the surface will be attracted to it and thereby lost.¹¹ The net effect of such a situation, of course, would be to reduce the effective orifice area for ion transmission.

Two experiments came to mind to test this "model." First, the neutral gas flow through the orifice is approximately proportional to the orifice area.¹² If, on the other hand, a "forbidden zone" for ion transmission exists near the perimeter of the orifice, the entering ion current

will not be proportional to the orifice area. Second, if such a "forbidden zone" exists, its extent will probably be a function of the orifice material and geometrical configuration.

A study was made of the dependence of the entering positive ion current as a function of the orifice diameter and sampling cell pressure. The results are shown in Fig. 4.

The lower curve shows the result obtained for a 110 micron diameter orifice, the same one used to obtain the data of Fig. 3. The line drawn through the solid measured points is simply a "French-curve" fit to the data. The open circle and open triangle data points were obtained by subsequently increasing the orifice diameter to about 150 and 310 microns, sequentially. This was accomplished by simply enlarging the hole diameter with miniature drills. This procedure was used in an effort to keep any other effects likely to be encountered in changing from one orifice size to another to a minimum.

The dashed curves situated near the data points for the 150 and 310 micron diameter orifices respectively were computed. That is, if it is assumed that the entering ion current for the larger orifices should scale upward from that obtained for the 110 micron orifice in the same way as the neutral gas flow scales, these curves would result. Mathematically, the expression used was

$$I(P, D) = I(P, d) \left[\frac{f(P, D)}{f(P, d)} \right], \quad (1)$$

where $I(P, D)$ and $I(P, d)$ are the entering ion currents for the large diameter (D) and small diameter (d) orifices, respectively, and $f(P, d)$ are their relative conductances.¹³ Thus by computing the conductance ratios and using the entering current curve $I(P, d)$ for the smaller orifice, the projected currents for enlarged orifices $I(P, D)$ were determined.

Within the combined uncertainties of the computations and the measurements, there is reasonable agreement between these measured and computed results. The conclusion to be drawn from such studies is that

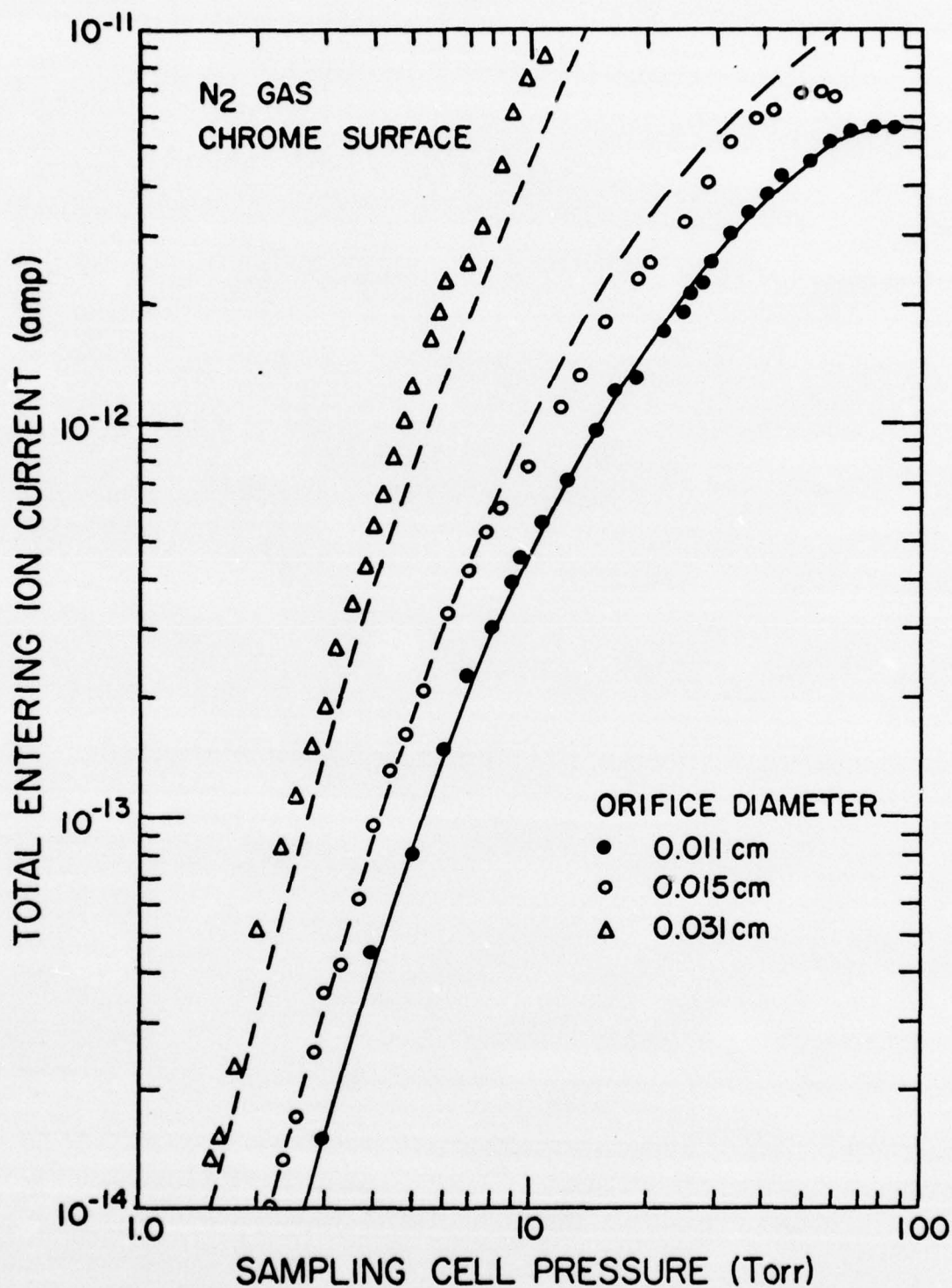


FIG. 4. Ion sampling current versus sampling cell pressure for three orifice diameters. The two dashed curves for the larger orifices are computed from the solid curve for the small orifice. See text.

the current of entering ions does scale, at least to within a reasonable approximation, to the orifice neutral gas conductance. Consequently, if there is a "forbidden zone" of the type discussed above, its extent must be rather small compared to the orifice area.

To substantiate this conclusion, another test was conducted. Two rather different orifices, but of about the same diameter, were investigated. One of these consisted of an orifice/orifice plate combination which had been plated to insure surface continuity; the other featured different materials. One had the features of a small hole in a very thin-walled sheet; the other was more like a short tube, or even a short tube in series with an aperture. One orifice was quite circular; the other somewhat more elliptical in shape. In short, the two were about as different as could reasonably be made and still preserve the basic overall features of the typical orifices shown in Fig. 2.

Within the limits of our ability to compute the neutral gas conductance of these orifices, the ion current entering the high vacuum system was directly proportional to the neutral gas flow. Once again, therefore, the concept of a "forbidden zone" did not appear probable, i.e., there was little evidence to support the suggestion that the rapid fall-off of the sampling ion current had anything to do with any sort of surface phenomenon, at least in terms of its gross features.

In an attempt to gain some understanding as to how the effect of small potentials on the orifice surface might affect the ion transmission, studies of the type presented in Fig. 5 were undertaken. Here is plotted the current of ions traversing the orifice as a function of the orifice plate potential relative to the remaining walls of the sampling cell.

Note that the positive ion current passing through the orifice goes through a maximum at an orifice plate potential of about 0.25 volt. (Caution should be taken here in that there may be a contact potential difference of up to about 0.5 volt between the actual potential of the orifice plate surface and that applied to this electrode.) For more

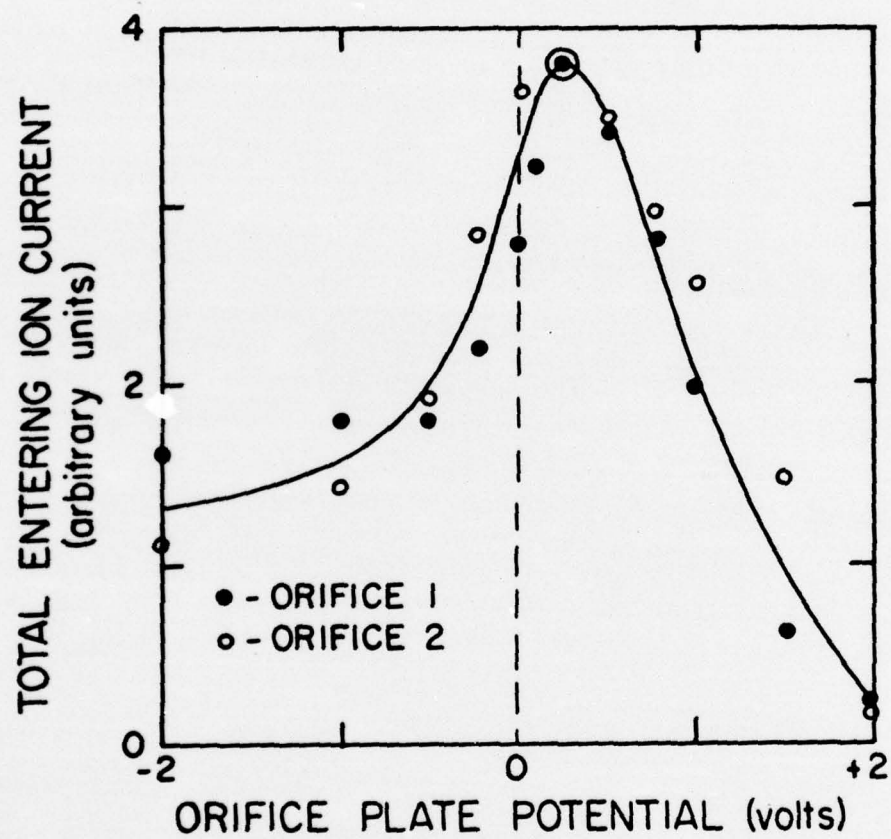


FIG. 5. Ion sampling current versus orifice plate potential

positive orifice plate potentials, the ion current drops rapidly, approaching zero at about +2 volts. This phenomenon is interpreted as the inability of the positive ions to overcome this motion-retarding potential barrier as the neutral gas flow pushes them towards the orifice.

On the other hand, application of a negative potential to the orifice plate should draw positive ions towards the plate. In fact, it does, but this also results in a decreased transmission. A detailed consideration of the electric field lines in the vicinity of the orifice itself indicates that the field lines terminate on the orifice edge. Thus as the ions approach the orifice, they are accelerated towards this edge and are lost at the surface as they are moving through the orifice. Hence only those ions approaching the orifice near its axis (where the edge forces are approximately balanced) will get through. These more or less "centered" ions are felt to be responsible for the "tail" on the entering ion current extending to larger negative orifice potentials.

It thus appears that the maximum ion orifice transmission occurs at or near zero potential relative to the "at rest" potential at which the ions are formed. Furthermore, small deviations on the order of a few tenths of a volt from this value do not have gross effects of the ion orifice transmission.

A final example of the type of parameter study which was undertaken during the early part of these investigations is the result shown in Fig. 6. As mentioned near the beginning of this section, the Faraday cup ion collector located just inside the orifice plate was fronted by a fine-screen grid. Fig. 6 shows the effect of the potential applied to this grid on the collected ion current.

Note that, for negative grid potentials, the positive ion collector current is constant beyond about -10 volts. Here almost all the ions entering the high vacuum system through the orifice are passing through the grid¹⁴ and being collected by the Faraday cup. As the potential is allowed to approach zero, the collector current drops slightly, as some

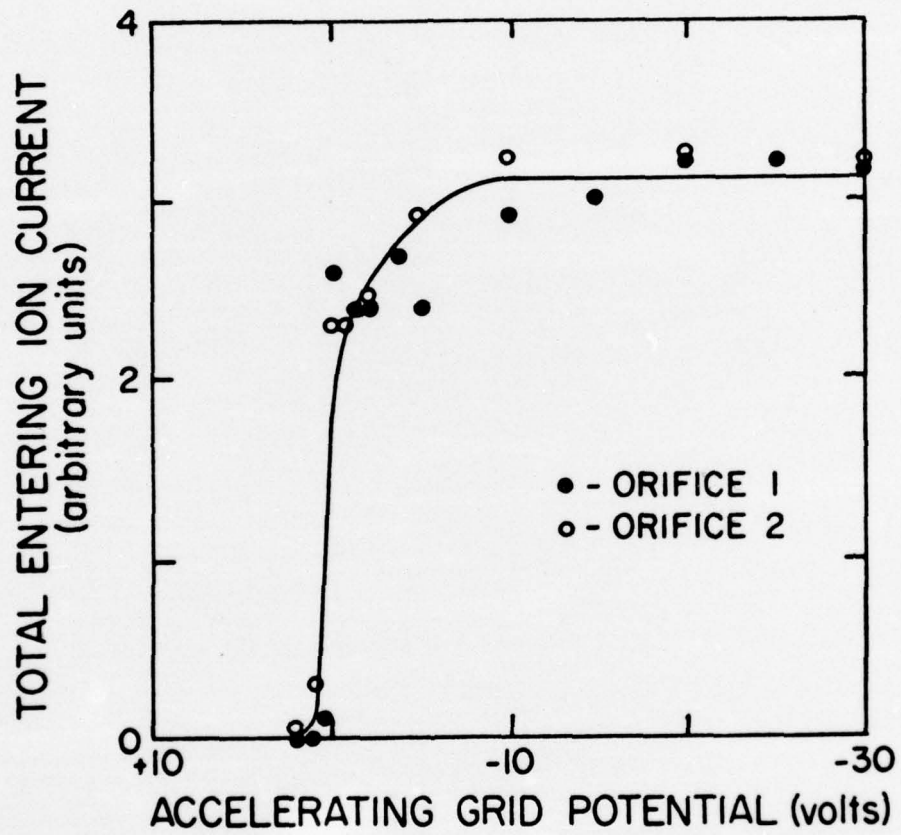


FIG. 6. Ion sampling current versus accelerating grid potential

of the entering ions, being now almost totally controlled by the flow of the expanding neutral gas, reach a sufficient "off-axis" position to elude the Faraday cup. However, at or very near to zero grid potential, the collector current drops abruptly to essentially zero. This indicates that few, if any, of the entering ions have high kinetic energy as, if they did, they would be able to overcome this retarding potential on the grid. The conclusion was that the entering ions are essentially at thermal energy as they negotiate the orifice.

On the basis of the data presented in this section and the results of other similar type studies, several preliminary conclusions were made. First, it did not appear that the choice of orifice material was of critical importance for the overall ion sampling efficiency. Second, the ion current passing through the sampling orifice seems to scale approximately with the neutral gas flow conductance of the orifice, i.e., the ion and neutral flow efficiencies were about the same over the pressure range investigated. Finally, small electrosurface or contact potential effects should not result in gross changes in the total ion sampling efficiency.

Thus, in a sense, the sampling system itself appeared to be operating in the way it was intended to operate. Rather than simply extending the types of measurements presented here to other orifice materials and/or orifice geometrical configurations, it was decided to look in more detail at the "expected" sampling current. Indeed, there was little point in spending great amounts of time in attempting to improve the overall system efficiency if it were already near its optimum. This decision grew into the material now presented.

IV. ANALYSIS OF THE ION SAMPLING RATE

As mentioned in the last section, the current of ions entering the high vacuum region from the sampling cell was about 1/2 of that expected in the pressure range above about 40 Torr. In this section, the procedures used to make such crude estimates of the expected entering current are

first reviewed. A somewhat more detailed analysis of the equilibrium ion density in the sampling cell is found in the latter part of this section.

In the ion sampling cell of the laboratory ion sampling apparatus (see Fig. 1), ions are created by alpha particle bombardment of the sampling cell gas. As mentioned in Section II, the Am^{241} alpha source has an activity level of 700 microcuries producing about 2.6×10^7 alpha particles/sec. For purposes of computation, it has been assumed that this flux is emitted isotropically in the hemisphere, i.e., in the 2π steradian solid angle available from the plane of the source. Thus the alpha particle flux is given by

$$F_{\alpha}(r) \approx \frac{2.6 \times 10^7}{2\pi r^2} = \frac{4.1 \times 10^6}{r^2} \text{ } \alpha\text{'s/cm}^2\text{sec}, \quad (2)$$

where r is the distance from the source.

For an alpha particle energy of about 5.5 meV, the ionization efficiency in air along a path is

$$R_{\alpha} \approx 2.0 \times 10^4 \text{ ion pairs}/\alpha \text{ cm atm.} \quad (3)$$

The volume rate of ion and electron formation is thus

$$\left(\frac{dN^+}{dt}\right)_F = \left(\frac{dn^-}{dt}\right)_F \approx F_{\alpha} R_{\alpha} P(\text{atm}), \quad (4)$$

where P is the pressure in atmospheres. Using the results of equations (2) and (3) and converting the pressure to Torr gives

$$\left(\frac{dN^+}{dt}\right)_F = \left(\frac{dn^-}{dt}\right)_F \approx \left(\frac{1.1 \times 10^8}{r^2}\right) P_0 \text{ ion pairs/cm}^3 \text{ sec}, \quad (5)$$

where P_0 is in Torr.

Most of the ion sampling current measurements undertaken were made with the alpha particle source about 2 cm from the orifice. Thus if the pressure dependence of equation (5) holds down into the 2 Torr

region (this point will be discussed in more detail later), of order 5×10^7 ion pairs/cm³-sec were being produced in the vicinity of the orifice.

The ionic species produced in the ionization are probably mostly electrons and molecular ions. At pressures in excess of 10 Torr or so, the primary mechanism for loss of the ions produced by the alpha particle ionization is positive ion-negative charge recombination. The recombination rate w , for electrons and positive molecular ions (dissociative recombination) is typically 2×10^{-7} cm³/sec. Recombination rates for positive ion-negative ion recombination are of comparable magnitude, so the conversion of electrons to negative ions (by some attachment process) should not appreciably alter the recombination rate. Because of the large magnitudes of these rates, three-body recombination does not drastically alter the net recombination occurring in the system.

Since the net ion loss rate should be recombination dominated in this pressure range, neglecting all but this simple effect gives

$$\left(\frac{dN^+}{dt} \right)_L \approx w N^+ n^- \approx w [N^+]^2, \quad (6)$$

where N^+ and n^- are the positive ion and electron (or negative ion) densities, which are of the same magnitude. If this approximate ion loss rate is now equated with the ion formation rate of equation (5), i.e.,

$$\left(\frac{dN^+}{dt} \right)_F = \left(\frac{dN^+}{dt} \right)_L, \quad (7)$$

one finds

$$N^+ \approx 1.2 \times 10^7 P_o^{1/2}. \quad (8)$$

At a sampling cell pressure, for example, of about 50 Torr, the equilibrium ion density N^+ is thus about 8.5×10^7 ions/cm³. If 1 cm³ of gas is being conducted through the orifice per second, (i.e., a 1 cm³/sec orifice conductance) an ion current of about 1.3×10^{-11} ampere should be flowing through the orifice assuming none of the ions in the 1 cm³ volume

are lost in the process. The conductance of the 0.011 cm diameter orifice which was used to obtain the ion transmission vs. pressure data of Fig. 3 is, in fact, about $1 \text{ cm}^3/\text{sec}$. The expected ion current of about 1.3×10^{-11} ampere at 50 Torr is about twice the observed value of 5×10^{-12} ampere. This kind of agreement is certainly within the accuracy of the crude computations made (particularly since including three body recombination and a more detailed analysis of the ion reactions suggest the "expected" current is about a factor of 2 high).

Of course, in this high pressure region, the mean-free-path for atomic collisions is very short, and is much smaller than the orifice diameter ($\lambda \ll \text{dia.}$). Here the ion motion should be rather completely dominated by collisions with the neutral gas molecules. Thus the ions should flow through the orifice along with the neutral molecules and few are likely to be lost during this transit.

Note that equation (8) says that the ion density in the sampling cell goes as the square root of the cell pressure. If the pressure is reduced from 50 to 5 Torr, the ion density should only go down by a factor of 3 or so. Fig. 3, on the other hand, indicates an ion current drop of about 2 orders of magnitude for this pressure change. The initial interpretation of this discrepancy was that the "ion transmission efficiency" was a rapidly falling function of decreasing pressure.

Some time was spent trying to understand this phenomenon. Forbidden zones (of the type described in the last section) were postulated for ions close to the cell or orifice plate walls. It was recognized that diffusion to the walls would be a serious problem in the vicinity of the walls and various diffusive (and as mentioned, electrosurface) effects were invoked to explain this rapid decrease in ion sampling efficiency. This effort was underway at the same time that the results described in the last section were being obtained.

One of the early tests which gave some insight into the nature of the problem was the fact that, when measurements of the type presented

in Fig. 3 were made with negative ions, the drop-off of ion current with pressure was even faster than for positive ions. (No attempt was made in these studies to separate negative ions from electrons.) This and other observations suggested that our simple-minded model for computing the expected ion concentrations in the sampling cell was insufficient to give even an approximate ion density in the cell below about 10 Torr.

One of the keys to interpretation of the ion sampling vs. pressure curves such as shown in Fig. 3 was found in consideration of the fate of the electrons which were produced in the initial alpha particle ionization collisions. Three basic mechanisms can be suggested to explain the loss of these electrons; namely, electron-positive ion recombination, negative ion formation, and diffusion to the walls. While the diffusion of ions was not considered to be of great significance in the 10 Torr region, the diffusion of electrons cannot be ignored as their diffusion coefficient is some orders of magnitude larger than that for ions.

By taking some typical values for recombination rates between ions and electrons (including three body) and typical values for some electron attachment rates to form negative ions (again, three body) it was possible to compute the "electron residence times" in the sampling cell against these loss mechanisms. That is, how long will an electron remain free and unattached? It was also possible, using an electron diffusion coefficient given by¹⁵

$$D_e \approx 10^6 / P_o, \quad (9)$$

to compute the electron residence time against diffusion in the cell. The results of one such computation are shown in Fig. 7.

Note that for pressures above about 10 Torr, the electron residence in the cell is limited by negative ion formation. On the other hand, at lower pressures, the electron residence time is diffusion limited. Interestingly, the electron residence time for ion-electron recombination (which are ion density dependent) do not limit the residence time at any pressure.

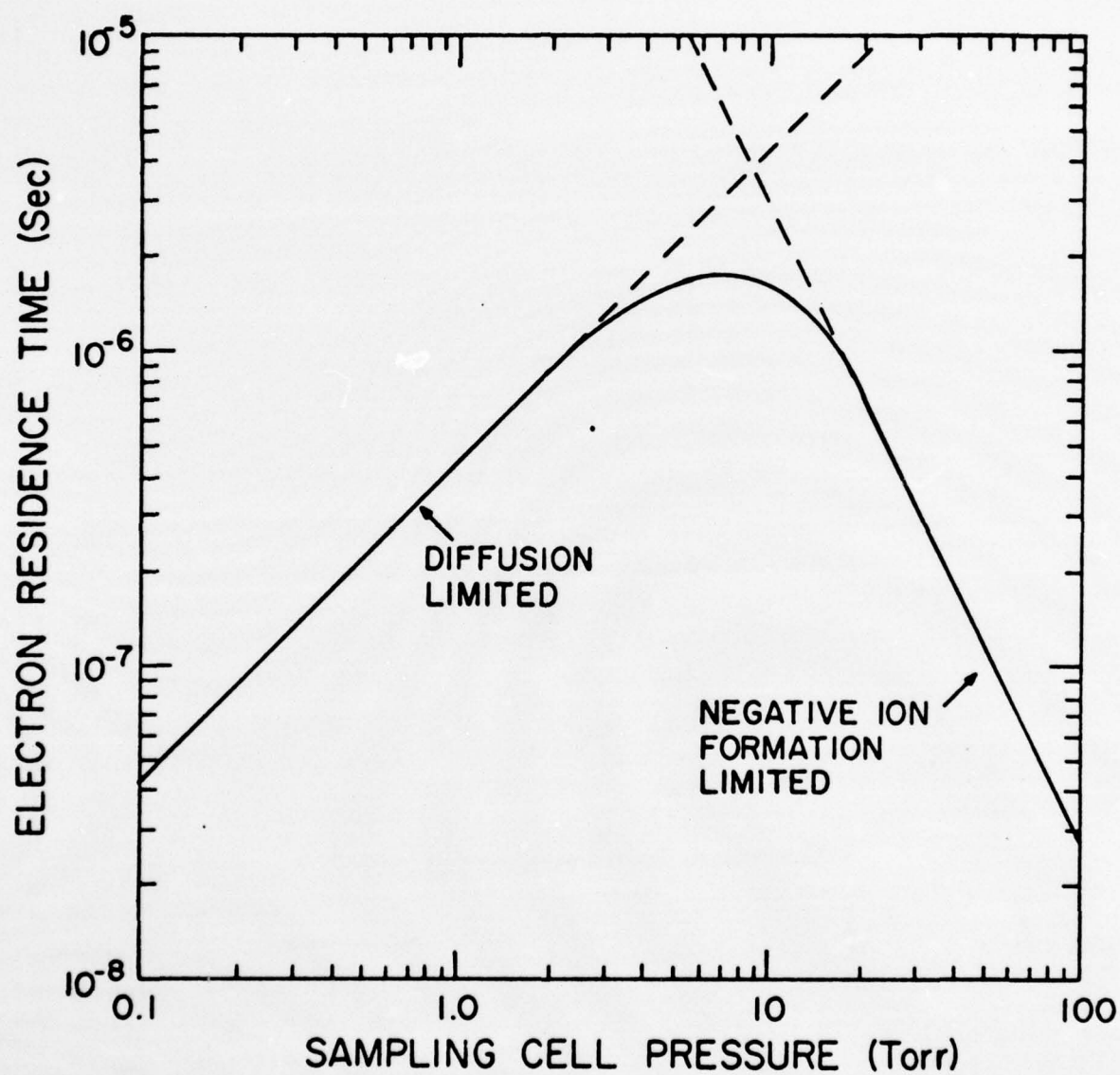


FIG. 7. Electron residence time in the sampling cell versus cell pressure

In the region between about 2 and 20 Torr, the electron residence time is controlled by both diffusion and negative ion formation as approximated by the heavy line in Fig. 7. Results of calculations such as these are not to be taken as accurate by any stretch of the imagination. Indeed, they are dependent on the cell dimensions and configuration (diffusion) and by the gas purity (attachment). Nevertheless, the data should give an approximate identification as to the fate of the initial electrons.

The trend of the data in Fig. 7 is, in fact, of considerable significance. At the lower pressures, these results indicate that the electrons diffuse away very rapidly. If the electron densities are restricted by this diffusion loss, the positive ions must also be diffusion limited as there are no negatively charged particles around for them to recombine with. Thus, even though the diffusion coefficients for ions are orders of magnitude less than for electrons¹⁵, diffusion must still play an important role in the ion density determination in the sampling cell.

Positive ion residence times were also computed. These results are not shown as they are even more approximate than those for electrons. The general features of the results, however, are very similar to those of Fig. 7, i.e., ion residence times are recombination limited above about 10 Torr and diffusion limited at lower pressures. Maximum residence times on the order of 0.01 to 0.1 sec are found in the 10 Torr region, as compared to the much smaller 10^{-6} sec residence times for electrons at this pressure.

Thus it appears that the simple computation of the sampling cell ion densities (assuming recombination as the only loss mechanism) are not valid at 10 Torr and even less valid at lower pressures. In fact, the actual computation of ion densities in the cell must be made from the relationship

$$\left(\frac{dN^+}{dt}\right)_{\text{Formation}} = \left(\frac{dN^+}{dt}\right)_{\text{Loss by Diffusion}} + \left(\frac{dN^+}{dt}\right)_{\text{Loss by Recomb.}} \quad (10)$$

This equation can be written as

$$KN_o = -D_+ \left(\frac{d^2 N^+}{dx^2} \right) + (w_{2B} + w_{3B} N_o) N^+ N^-, \quad (11)$$

where N_o , N^+ , and N^- are the neutral, positive ion, and negative ion densities, D_+ is the ion diffusion coefficient, and w_{2B} and w_{3B} are the net 2 and 3 body recombination rates and K is a constant.¹⁶ Note that the diffusion term contains only the x coordinate derivative and that only one species each of neutrals and ions has been allowed. Even in this gross approximation, however, equation (11) is second order nonlinear in N^+ and cannot be rigorously solved.

On the other hand, if either the diffusion or recombination loss terms can be set to zero, a solution is possible. From data of the type presented in Fig. 7, an estimate of the range of validity of these approximations can be obtained. Thus, for pressure in excess of about 20 Torr, diffusion can be ignored and N^+ and N^- should be comparable. Then

$$N^+ = \left[\frac{KN_o}{w_{2B} + w_{3B} N_o} \right]^{1/2}, \quad (12)$$

a solution very similar to the initial estimates made in the pressure range above about 40 Torr except that three body recombination has been included.

In the region below about 2 Torr, the recombination term can be ignored and the solution becomes

$$N^+(x) = 1/2 \left(\frac{KN_o}{D_+} \right) [d^2 - x^2] \quad (13)$$

where x is the coordinate measured along the axis of the ion sampling system (see Fig. 1) from the cell center ($x=0$) and d is the distance from the cell center to the front of the orifice plate.¹⁷ Note that $N^+(x)$ is a parabola,¹⁸ with the largest N^+ occurring at the cell center as expected.

Thus at low pressures, the positive ion density in the cell is parabolic in coordinate x with its maximum at the center of the cell. As the pressure is increased, the recombination limited value given by equation (12) is reached, at which time the ion density becomes approximately constant over the center portion of the cell. As the pressure continues to increase, this "constant density" region expands to fill most of the sampling cell volume.

In the low pressure regime, the flux of ions reaching the orifice plate front surface is given from diffusion theory as

$$J(x) = -D_+ \left(\frac{dN^+}{dx} \right)_{\text{at } x=d} \quad (14)$$

Using equation (13) for N^+ and evaluating leaves

$$J(x) = KN_o d. \quad (15)$$

If the assumption is now made that if an orifice is present in this plate and flux $J(x)$ is incident on the orifice area, these ions will go on through the orifice, the entering ion current will be

$$I^+ = e (KN_o d) (\pi a^2), \quad (16)$$

where πa^2 is the orifice area and e the electronic charge unit.

In this low pressure limit, the motion of the ions is entirely in the $\pm x$ direction in our model. Thus the only ions which can traverse the orifice are those in a "tube" having the same diameter as the orifice and extending into the cell from the orifice plate.

This is, of course, an approximation. In fact, the presence of the orifice in the orifice plate gives rise to a pressure gradient radially towards the orifice from every point in the cell. There is therefore a net velocity of the gas molecules in a direction towards the orifice. It is only under the conditions that the diffusion velocity in the x direction is much larger than the radial pressure gradient flow velocity that equation (16) is valid. While the procedures used were only approximate, it was estimated that this condition was reasonably satisfied so long as the pressure was below about 1 Torr.

On the other hand, at pressures above about 20 Torr, the pressure-gradient-generated flow velocity of the neutral gas molecules is substantially larger than the now much-diminished diffusion velocity. Thus, as in our earlier simple model, the ion motion is dominated by the neutral gas flow and, for a $1 \text{ cm}^3/\text{sec}$ conductance orifice, about 1 cm^3 of gas from the hemisphere around the orifice enters the system carrying the ions along. The entering ion current is thus

$$I^+ = e f(P) N^+, \quad (17)$$

where, as before, $f(P)$ is the orifice conductance.

The computations made with equations (16) and (17) for the entering ion current are compared with that measured for O_2 gas with an 0.031 cm diameter orifice in Fig. 8. (Oxygen was used for many studies as it readily forms negative ions, and the effective recombination rates can be better estimated than for a sample in which most of the negative ion formation must come from impurities.)

Note that in the 40 to 50 Torr region, the measured entering current is approaching the value computed assuming the ion densities in the sampling cell are recombination limited. Below this pressure, however, the measured current drops rapidly and appears to be approaching the lower curve in the 2 Torr region, the region where this diffusion limited sampling cell ion density should begin to become applicable. It is worth noting that, while the computed curves are quite approximate in absolute value, the results shown here are absolute, and have not been normalized to the measured results.

It thus appears that the rapid fall-off of the entering ion current can be largely attributed to "bridging the gap" between the pressure regions where the ion densities in the sampling cell are dictated by these two phenomena.

The shape of the entering ion current-versus-pressure curve will certainly be a function of the apparatus used for the measurements. As such, these results need not apply to the situation occurring in the atmosphere

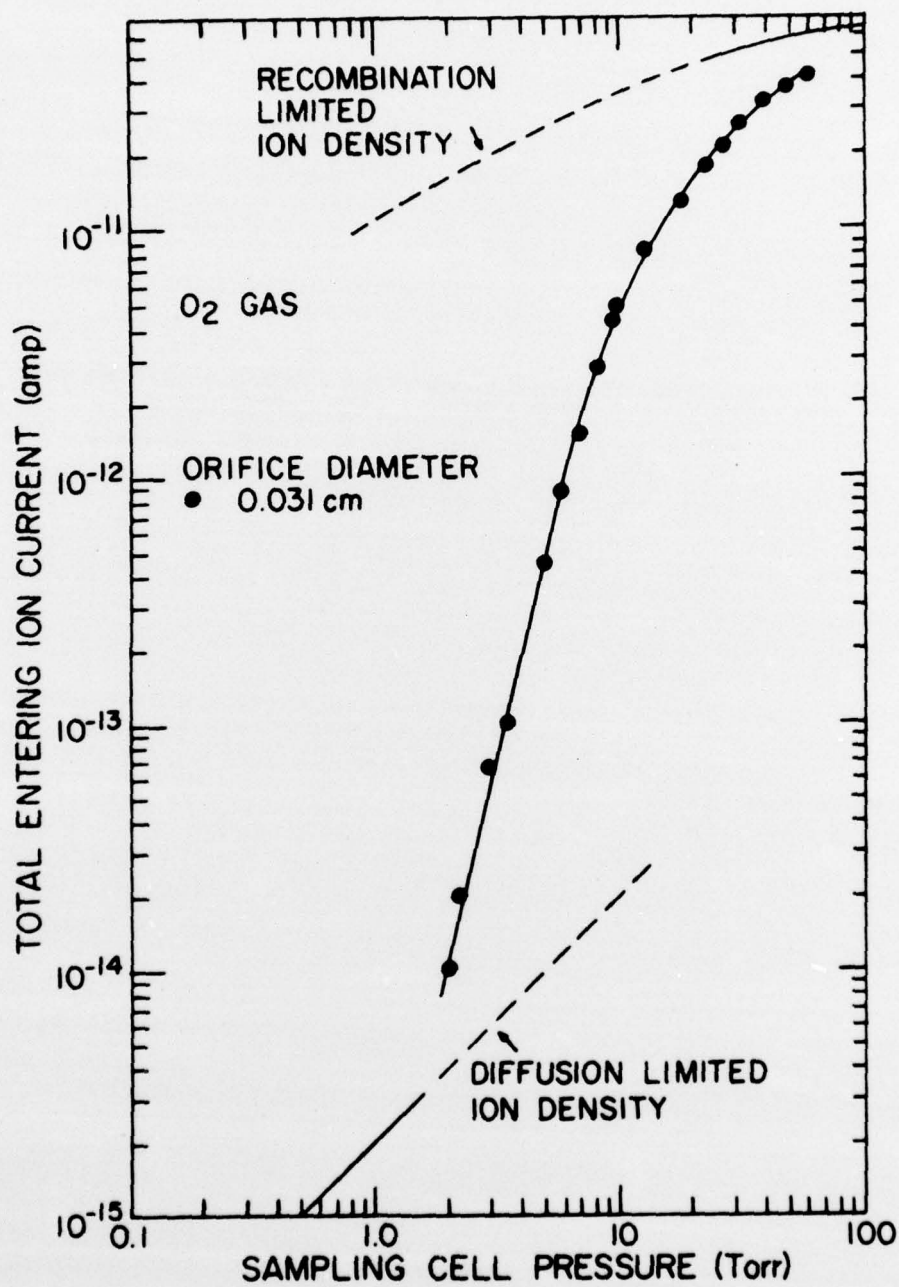


FIG. 8. Ion sampling current versus sampling cell pressure

with the actual flight instrument. On the other hand, there appears to be little question that diffusion effects may have a significant influence on the stratospheric measurements, a point which will be discussed in more detail in Section VI.

The shape of this curve may also be affected by other phenomena. For example, the alpha particle ionization process may not depend on pressure according to equation (5). As much of the total ionization from such a technique stems from secondary electron production (i.e., where the primary electrons produced have sufficient energy to further ionize the target gas), the range of the primaries becomes important. At lower pressures, these initial electrons may encounter the cell wall before producing additional ionization.

Wall effects have also been ignored. That is, secondary electrons from alpha particle-wall collisions could be having an influence on the measured currents. Various electrode configurations were employed in the ion sampling cell to test for some of these potentially troublesome effects. While these tests were never completed, these workers found nothing which would seem to invalidate the results presented.

Nevertheless, these workers present the data of this section with considerable hesitancy. It must be stressed that the thoughts presented are only of a preliminary character. Many troublesome problems exist and were simply not properly evaluated because of lack of time. The model presented to explain the observed results contains many uncertainties and, while giving a reasonable answer, can hardly be regarded as verified. In short, this model must be regarded only as "a possible explanation" at this time.

In addition, these workers are not willing to conclude that the shape and material of construction of an orifice will have negligible effect on the overall sampling efficiency. Factor-of-2 kinds of differences could easily be possible for variations of this kind. Nevertheless, it seems unlikely that the gross features of the entering ion current-versus-pressure curves presented here can be attributed to such effects.

V. THE ION OPTICAL SYSTEM AND QUADRUPOLE MASS SPECTROMETER

The ion optical system which was developed to bring the ions from near the sampling orifice to the quadrupole mass spectrometer/particle multiplier detector was presented in Fig. 1. This electrode arrangement was found to be easy to construct and keep in alignment, to have a large ion transmission efficiency, and to be operable with some of the same voltages required elsewhere in the flight instrument package.

Note first the region between the back side of the orifice plate and the ion accelerating aperture. The electric field in this region is similar to that between a flat plate and a cone in another flat plate. Here the equipotential surfaces tend to flare down into the cone recess. This gives rise to a force on an entering ion which always has a component towards the axis of the system. Thus, this arrangement of these two electrodes is basically a focusing configuration. It was typical to operate the ion accelerating electrode at a potential of 10 volts relative to the orifice plate. Keeping this accelerating potential small is important from the viewpoint of preventing the cluster ions entering the apparatus in the stratosphere from being dissociated in high-energy collisions.

The combination of electrodes formed by the ion accelerating aperture, the ion focusing electrode, and the quadrupole entrance aperture have rather similar features to an Einzel lens.¹⁹ By application of a potential to the ion focusing electrode, the ions coming through the ion accelerating aperture can be made to focus on the quadrupole entrance aperture. As is the case with an Einzel lens, the ion focusing electrode can be operated in either an accelerating or decelerating mode, depending on the potential applied. In general, lower applied potentials (and thus lower ion energies) lead to the decelerating mode operation which is used here.

Under reasonable operating conditions, 65 to 70% of the entering ions can be made to enter the quadrupole mass spectrometer. This highly efficient system is accomplished, as mentioned above, with application of potentials which do not exceed 10 volts, a fact which should keep cluster dissociation to a minimum.

The ion-optical system which was developed for this laboratory ion sampling apparatus was so successful that it was incorporated directly into the second flight instrument package.

The quadrupole mass spectrometers used for this study and for the actual flight measurements are commercially available instruments.²⁰ Here again, the actual flight quadrupole was tested, together with the ion optical system described above, in the laboratory facility. In general, it was found to be far easier to accomplish such evaluations in this test apparatus than in the actual flight instrument which was designed for in-flight specifications (convenience of laboratory operation not being such a specification).

As an example of the mass-scan data obtained with this apparatus, the data of Fig. 9 are presented. These results, taken with a room air sample, were rather surprising to these workers in that not a single trace of the primary ions (which must have been N_2^+ , O_2^+ , etc.) remain amongst the sampled ions. In fact, many of the peaks shown were also present when runs were made with "pure" Ar targets, and are probably the result of vacuum line impurities.²¹

The hydrated proton peaks of mass 55, 73, 91, and possibly 109 amu are tentatively identified as the first 4 peaks. The large mass peak at about 300 amu is not identified.

On another occasion, when the system was operated immediately after some new electrodes had been installed in the ion sampling cell, the only peak present in the mass scan was about mass 115 to 120 amu. While identification was not positive, it was remembered that just prior to installation, the new electrodes had been cleaned in acetone (CH_3COCH_3), and an acetone ion-neutral molecule cluster (mass 116 amu) could be responsible for the ion observed.

The point of presenting such results is to show that cluster ions, even though their species is unknown, are able to survive as clusters during the sampling process. The masses 55 to 109 amu shown in Fig. 9 are only bound by typically 0.5 eV energy. Nevertheless, they seem to have survived the sampling process quite well, and there is little reason to doubt that a similar situation will occur in the stratosphere.

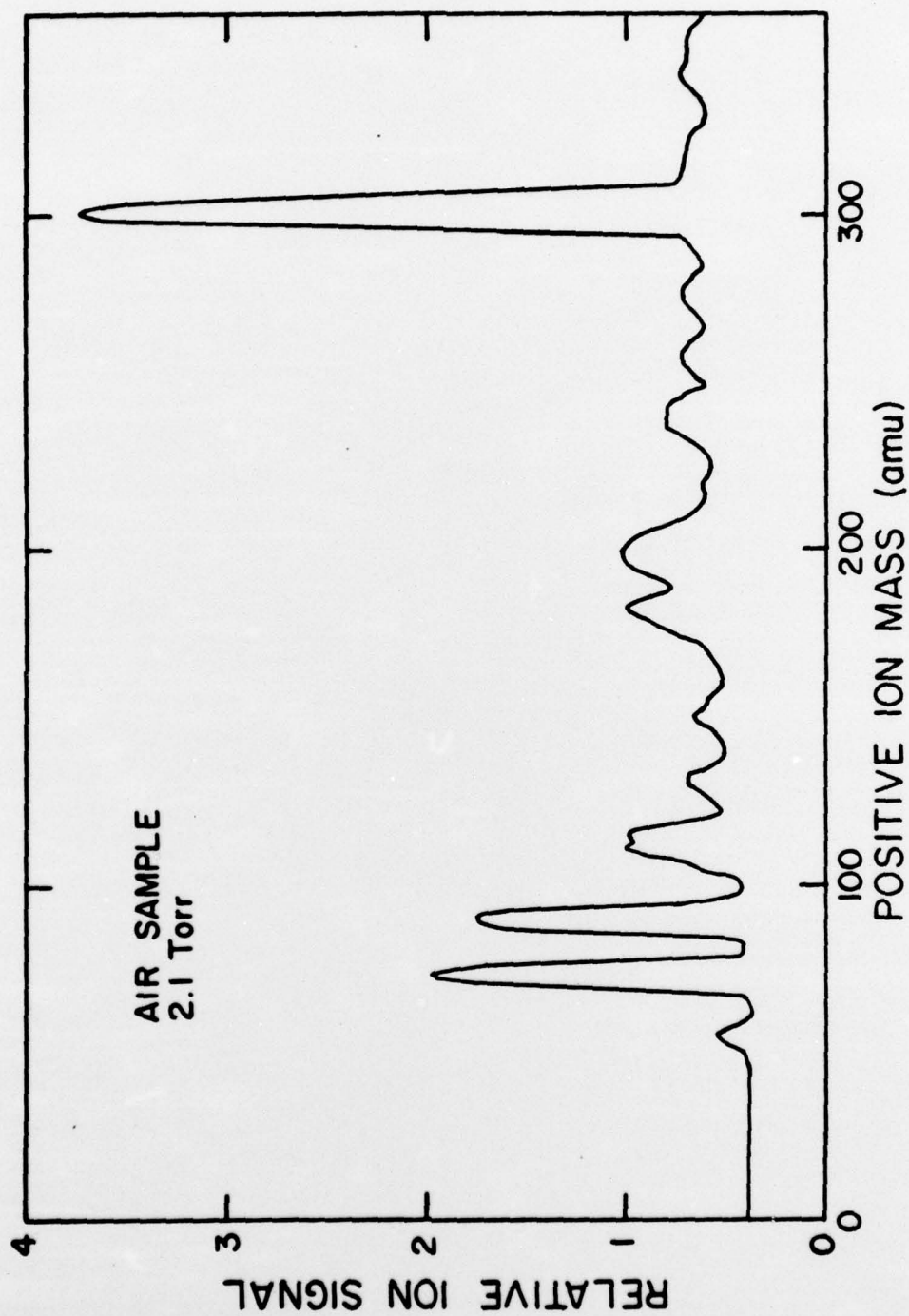


FIG. 9. Positive ion mass scan for 2.1 Torr room air sample

VI. SUMMARY AND DISCUSSION

At the time the proposal for these studies was written, the "low ion sampling efficiency" which had been observed during laboratory testing of the flight mass spectrometer package was attributed to an inability on the part of the ions to survive traversal of the ion sampling orifice. It was thus proposed that a study of ion transmission through small orifices be conducted for a variety of orifice sizes, configurations, and materials of construction.

Preliminary studies, made with the laboratory ion sampling apparatus built up for this investigation, indicated that the "low sampling efficiency" was not primarily the fault of any poor choices of orifice diameter, configuration, or material. This discovery changed the course of the present research effort which was to provide laboratory support data for the University of Denver stratospheric ion density measurement program.

A somewhat detailed analysis of the rates of production and loss of ions in the sampling cell was undertaken. It was shown that the ion loss mechanisms of importance are recombination at higher pressures and diffusion at lower pressures. The results of some crude calculations and some ion sampling measurements are presented to support the model discussed.

The research effort was concluded by the design and testing of suitable ion optics for use in the flight instrument package. A simple and yet highly efficient system resulted from these efforts and was shown to be compatible with the quadrupole mass spectrometer to be used during the stratospheric measurement program.

A fundamental question pertaining to the sampling of ions from the stratosphere has been raised by these studies. If the model suggested here for explaining the "low ion sampling efficiency" in the laboratory apparatus is correct, the role played by ion diffusion in the sampling process is of critical importance. As such diffusion effects are very dependent on the

geometry of the sampling system, the present laboratory apparatus is poorly suited to evaluate the effects of diffusion likely to occur in the atmosphere.

For the flight instrument, the ion sampling orifice lies in the center of a large metal "plane" which is facing downward. If there is no motion between the instrument package and the surrounding medium, the ion densities in the vicinity of the orifice will undoubtedly be significantly reduced by diffusion. On the other hand, the motion of the residual atmosphere up, down, or sideways relative to the package will each change the diffusion loss and thus the overall ion sampling efficiency.

Many of the above atmosphere-package relative motions could be simulated in the laboratory by "blowing" air at a large plate containing the orifice. Unfortunately, the present apparatus is not nearly large enough to accommodate such experiments, having been designed for a different type of measurements.

Nonetheless, it appears that the role played by diffusion in the stratospheric ion density measurements must be clarified if the results of the measurements are to be quantified.

Thus the laboratory ion sampling study has made some important contributions to the overall stratospheric measurement program. First, an efficient ion optical system was developed for the flight instrument and was tested, together with the mass spectrometer/particle detector, under conditions comparable to those used in flight. Second, it was shown that the orifice ion transmission is not strongly orifice configuration or orifice material dependent and varied approximately as the neutral gas flow conductance. It was also shown that the role of ion diffusion in the sampling process is substantial, and that efforts to fly at lower altitude (requiring more pumping speed) should be made as diffusion losses fall rapidly with increasing pressure.

Additional laboratory studies (both experimental and theoretical) on the effects of diffusion on the sampling process are needed if the results of any stratospheric measurements are to be placed on an absolute basis. It is probable that these authors will propose such studies when the results of upcoming stratospheric ion density measurements become available.

VII. APPENDIX

Crucial to the number of ions which can be sampled from the atmosphere or in the laboratory is the neutral gas flow conductance of the sampling orifices used. The techniques used for evaluating such conductances in this study are here reviewed.

The conductance through an infinitely thin-walled orifice of cross section area A in the molecular flow limit was deduced by Knudsen²² to be

$$f_{\text{MFL}} = 3.638A (T/M)^{1/2}, \quad (18)$$

where T is the gas kinetic temperature and M the molecular weight of the gas in amu.

It is, of course, not possible to construct an orifice in an infinitely thin wall; in fact, such orifices must be considered to be short tubes. A multiplicative factor K , the Clausing correction, must thus be incorporated into equation (18) of the form²³

$$K = \frac{1}{1 + t/2r} \quad (19)$$

where t is the wall thickness and r the orifice radius. Clausing factors K were only crudely determined for these studies due to the complexities of the orifice configurations used here, and generally ranged between about 0.5 and 1.0.

Liepmann²⁴ has investigated the dependence of the orifice conductance on pressure in the transition flow and viscous flow regions. These results, shown as the ratio of the orifice conductance to the orifice conductance in the molecular flow limit, are shown in Fig. 10, plotted against the flow Knudsen number (ratio of mean-free-path to orifice diameter). Note that Liepmann's results, the solid data points, trend smoothly from near 1.0 to 1.5 in the viscous flow regime.

The curve drawn through the data of Fig. 10 is the present fit to these data resulting from a conductance of the form

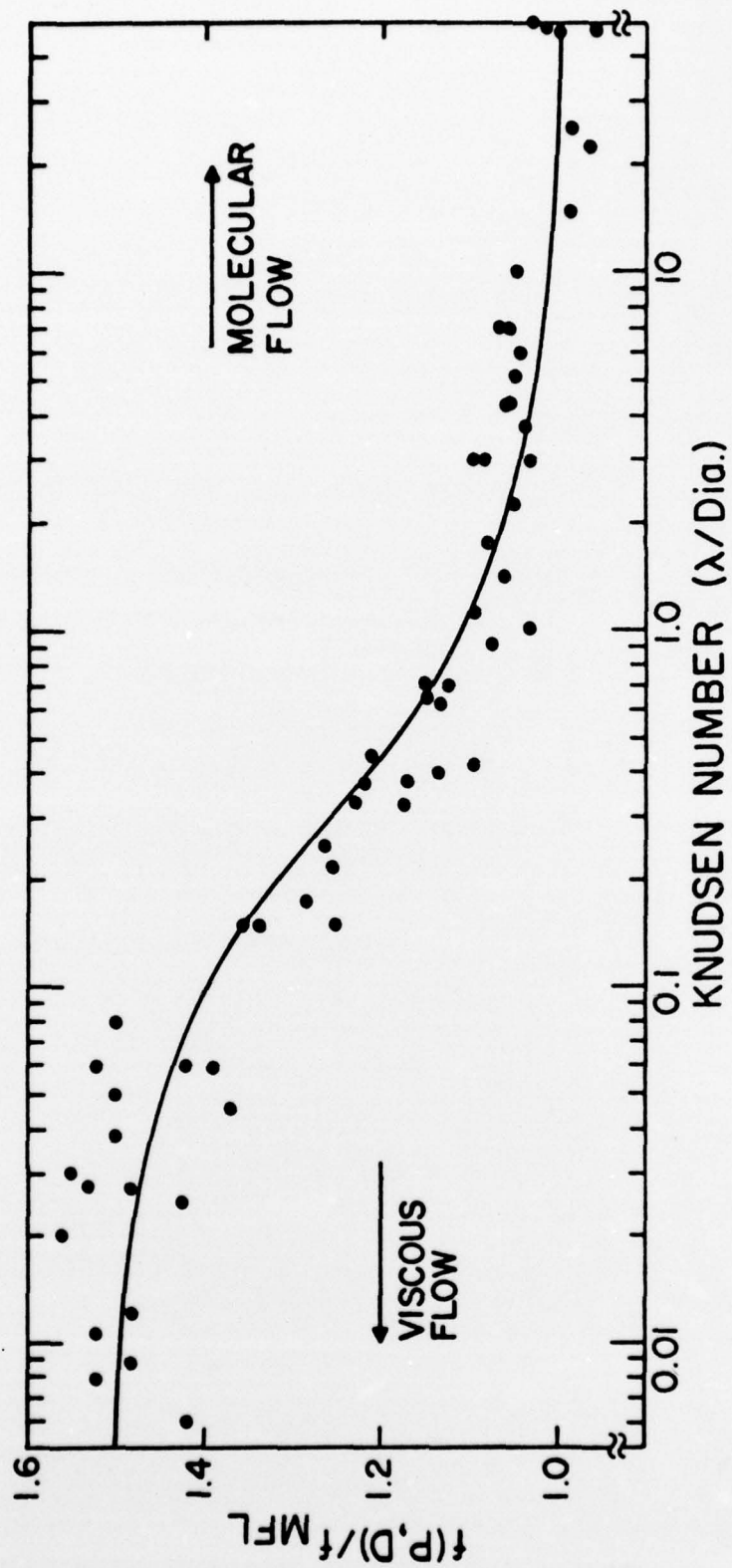


FIG. 10. Ratio of thin-walled aperture conductance to molecular flow conductance versus Knudsen number

$$f(P, r) = 5.56 \times 10^4 \left\{ 1 - 0.333(\lambda / r) [1 - e^{-r/\lambda}] \right\} Kr^2, \quad (20)$$

where the Clausing factor K has been set to unity. Equation (20) was used in the computation of conductances for the studies reported here.

VIII. REFERENCES AND FOOTNOTES

1. Support includes contracts from the Ballistic Research Laboratories and grants from the Army Research Office.
2. The first package was destroyed in a free-fall from 40 km.
3. D.G. Murcray and R.C. Amme, "Construction of a Balloon-Borne RF Quadrupole Mass Spectrometer Package", University of Denver Final Report on Contract No. DAAD05-73-C-0139, Dec. 1974.
4. For a recent summary of the ion densities and species expected in the stratosphere, see: G.E. Keller, "Final Report on Balloon-Borne, Mass Spectrometer Package for Studying Stratospheric Positive Ions and Neutral Molecules", BRL Report No. 1941, Oct. 1976.
5. Reference 4 contains a discussion of the other stratospheric ion density measurement programs which have been and are being conducted at this time.
6. Electron-beam machining was used to prepare these apertures.
7. It was necessary to employ very hard materials because of the vacuum sealing valve used on the flight instrument. This valve is described in F.E. White, Rev. Sci. Instru. 47, 641 (1976).
8. The orifice diameters were measured under a microscope but were only accurate to within about $\pm 10\%$ due largely to their slight asymmetries.
9. For these tests, a "sampling cell" was fitted to the flight instrument. The arrangement was quite similar to the present apparatus.
10. Such phenomena were found to occur at very low pressures (~ 20 millitorr) with an electron gun ionization source during very early studies made prior to these investigations.
11. It is here assumed that 100% of the ions which encounter a surface are neutralized and therefore lost.
12. The neutral gas flow conductance of orifices in the molecular flow, transition flow, and viscous flow pressure regions is the subject of the Appendix to this report.

13. Unfortunately, the enlarging of the orifice diameter by the techniques used resulted in a rather uneven hole with a "lip" in some places making estimates of the orifice diameter and the Clausing correction (see Appendix) rather uncertain.
14. The grid transmission was about 95%.
15. E.W. McDaniel, Collision Phenomena in Ionized Gases, John Wiley & Sons, Inc., New York, 1964. Diffusion coefficient data were also obtained from J. Dutton, J. Chem. & Phys. Ref. Data (NBS) Vol. 4, No. 3, 1975.
16. The authors have assumed that the densities of the charged particles in the cell are low enough so that ambipolar diffusion can be ignored.
17. To be rigorous, one dimensional diffusion can only be applied when the distance $2d$ (the cell depth) is much smaller than the cell diameter. For many of the measurements made, the cell depth $2d$ was reduced by insertion of an electrode in the cell to make $2d < \text{dia.}$, so that this condition might be better satisfied.
18. This crude analysis neglects various cell wall-boundary conditions. See for example, the discussion in Chapter 10 of Ref. 15.
19. An Einzel lens (after the German word single) is generally thought of as being composed of three apertures, the outermost two operated at the same potential.
20. Finnigan Instruments Corp.
21. Due to pumping limitations, the gas handling lines were not evacuated to below about 0.01 Torr.
22. M. Knudsen, Ann. Physik 28, 999 (1909), and 35, 389 (1911).
23. The Clausing factor correction is discussed in detail and referenced in B. Van Zyl, G.E. Chamberlain, G.H. Dunn, and S. Ruthberg, J. Vac. Sci. Technol. 13, 721 (1976).
24. H.W. Liepmann, J. Fluid Mech. 10, 65 (1961).

IX. PERSONNEL

The following is a list of participating scientific personnel involved in this research. No advanced degrees were earned relative to this project.

Robert C. Amme
D. Boyd Barker
David G. Murcray
Herschell Neumann
John R. Olson
Bruce R. Peterson
Harold L. Rothwell
Bert Van Zyl